Journal of Glaciology, Vol. 40, No. 134, 1994

Short-term velocity variations and basal coupling near a bergschrund, Storglaciären, Sweden

BRIAN HANSON
Center for Climatic Research, Department of Geography, University of Delaware, Newark, Delaware 19716, U.S.A.

ROGER LEB. HOOKE
Department of Geology and Geophysics, University of Minnesota, Minneapolis, Minnesota 55455, U.S.A.

ABSTRACT. Distance measurements using an automated electronic distance-measurement system in the north cirque of Storglaciären, Sweden, during the summer of 1989, revealed a diurnal variation in glacier speed. Amplitude and timing of the diurnal cycle correlate well with the timing and intensity of the diurnal temperature cycle, indicating that speed responds to variations in daily melt with a lag of approximately 4 h. One 2 d period of non-diurnal velocity variations corresponded with a large rainfall event. Finite-element modeling suggests that these velocity variations must be closely related to water inputs in the cirque rather than to longitudinal coupling with lower parts of the glacier.

INTRODUCTION

Glacier velocities can be measured readily only at the surface. Surface velocities, however, result primarily from strains near and at the bed. Basal coupling is influenced by water inputs to the bed, with variable time lags and variable horizontal coupling. This paper examines some aspects of short-term velocity variations near the headwall of the north cirque of Storglaciären, using a two-part approach: measured velocities and temperatures within the scale of the diurnal cycle provide estimates of the time lag, and finite-element modeling of the surface response to basal decoupling provides plausible limits on the length of horizontal coupling.

The sensitivity of the lower parts of glaciers to short-term variations in water input is now well established (e.g. Iken and Bindschadler, 1986; Hooke and others, 1989). In the present study, we have dealt with the highest region of a glacier, monitoring motions within a cirque a short distance from the bergschrund. Water inputs are smaller than on lower parts of the glacier because the melt rate is smaller, the probability of precipitation falling as snow rather than rain is greater and the catchment area above the bergschrund is smaller. The lag after water melts at, or falls on, the surface of a high cirque may be greater than in the ablation zone. During the late summer, much of the water at the surface in the ablation zone is carried into crevasses and moulins by well-established surface streams whereas, in the accumulation zone, water must still percolate through a substantial firn layer. One might thus expect that the smoother, slower water inputs to the cirque would be less likely to produce a discernible short-term effect on the velocity.

The bergschrund is an exception to the preceding generalizations about water inputs in the accumulation zone. Snowmelt and rainfall above the bergschrund follow a relatively short path to the base of the glacier, albeit at a point where the glacier is relatively thin. In the case of the north cirque of Storglaciären, the headwall area, projected on to a horizontal plane, is typically 100–200 m wide, and the snow-free parts of the headwall consist largely of bedrock rather than talus. Additionally, the dark, snow-free parts of the headwall efficiently absorb solar radiation and enhance the local melt. Within the cirque, the glacier surface is covered by the relatively bright snow of the previous winter throughout most or all of the melt season.

This paper reports on a series of measurements made in the north cirque of Storglaciären during the summer of 1989 for the purpose of determining whether the surface velocity near a bergschrund undergoes short-term velocity changes, and whether such changes could be correlated with plausible water inputs. Surface responses to changes in basal coupling are not expected to be direct or simple, but will be modified by the intervening ice (Balise and Raymond, 1985) and may be influenced by the longitudinal coupling with other parts of the glacier (Kamb and Echelmeyer, 1986). Since velocities on lower parts of this glacier have been studied extensively (Hooke and others, 1989; Jansson and Hooke 1989), we also wished to know whether the changes seen near the headwall are closely related to, influenced by, or an influence on changes further down-glacier. A series of finite-element model experiments was used to elucidate the coupling between changes at the bed at various locations beneath the glacier and surface velocities high in the cirque.

https://doi.org/10.3189/S0022143000003804 Published online by Cambridge University Press

VELOCITY MEASUREMENTS

Distance measurements

To determine whether short-term accelerations occur near a cirque headwall, we made detailed measurements of the velocity of a stake emplaced about 45 m from the bergschrund of Storglaciären (Figs 1 and 2). The measurements were made during a 3 week period in June and July 1989. Hooke and others (1989) presented a less detailed but longer (3 year) record of seasonal variations in velocity of Storglaciären and also gave references to earlier work on the glacier.

The primary short-term velocity data were collected using an automated electronic distance-measurement system (EDM) located on bedrock (Fig. 1). The target for the measurements was a triple prism mounted on a 6 m long stake, S30 (Fig. 1), drilled ~5.5 m into the snow (Fig. 2) at a location about 45 m from the bergschrund. Distance measurements were attempted every 10 min, with each measurement being the average of three readings by the instrument. Interruptions in the series were caused by poor visibility. The system was programmed to make repeated attempts to measure the distance when visibility was poor but was not always successful at resuming measurements after conditions had improved. Distance measurements were supplemented with angle measurements using a theodolite on days when wind and visibility permitted.

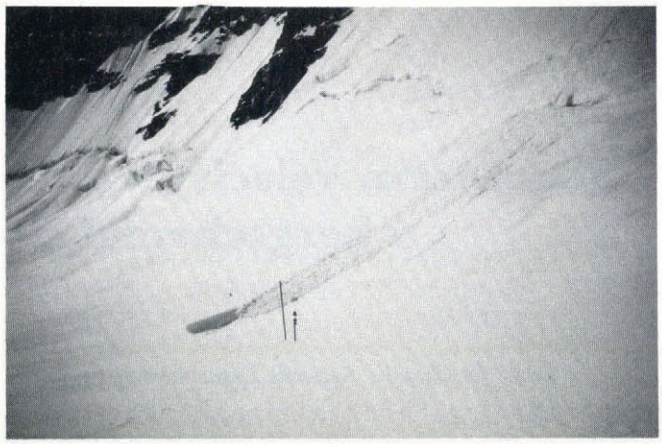

a

b

Fig. 2. Photographs showing stake used for automatic distance-meter measurements. a. View south showing proximity of stake to bergschrund. b. View north showing bergschrund in distance. Taller stake was used to assist in locating site from the ADM site.

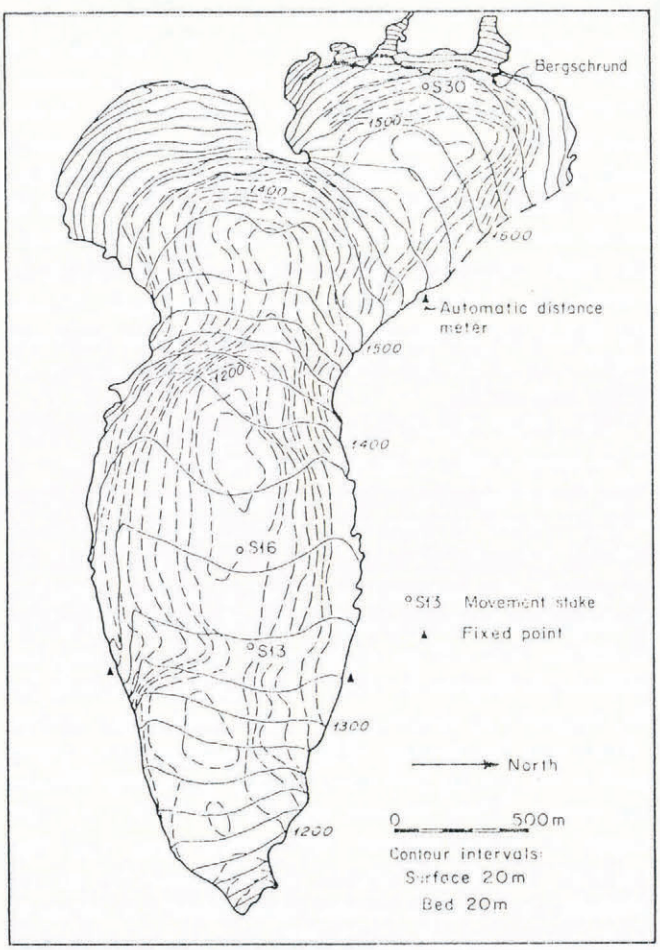

Fig. 1. Map of Storglaciären showing surface and bed topography, and locations of stakes and fixed points discussed in text.

Measurements commenced on 25 June 1989 and continued until 22 July 1989. Installation of an improved instrument shelter on 1 July caused the instrument position to be moved 9.3 cm farther from the prism.

The EDM has a stated absolute accuracy of 5 mm + 5 ppm, or about 9 mm in the current case. The relative accuracy of a series of measurements should be much better than this. Atmospheric corrections were applied using air-pressure and temperature measurements taken hourly at Tarfala field station, at an elevation 455 m below the measurement site. Temperature measurements, taken at a site between the instrument and prism, were available for atmospheric corrections from 5 July onward. Temperature and pressure measurements from Tarfala station were adjusted to the cirque elevation using an assumed lapse rate of 6.5°C km^{-1} and a form of the altimeter equation that included temperature corrections. The resulting corrections of the distance measurements varied from 17 to 28 mm, with half of the corrections falling into the range 21–25 mm.

Errors in these distance corrections could not have been responsible for the principal velocity variations to be discussed. The range of pressures and temperatures

https://doi.org/10.3189/S0022143000003804 Published online by Cambridge University Press

occurring over the period of measurement is such that changes in temperature would have had a greater effect than those in pressure, as pressure varied more slowly and has a lesser effect on the measurements. Temperature varied rapidly enough to have a significant effect on the apparent velocity only on certain sunny days during which shadows from the cirque headwall caused a strong diurnal cycle with an amplitude of up to 15°C.

The resulting data set consists of 1853 distance measurements over a 26.8 d period, with 29 gaps of more than 1 h in duration, four of which were more than 24 h. Of 17 theodolite measurements, the 13 taken after the fixed point changed comprise a consistent data set. During the 26.8 d period of distance measurements, the distance from the prism to the instrument decreased 535 mm, a rate of 19.9 mm d^{-1}. During the 21 d after the change in position of the instrument shelter, the actual velocity was directed 35.7° to the right of a line from the prism to the instrument site, as well as downward. Velocity components for that period were 15.0 mm d^{-1} horizontally down-glacier and 19.8 mm d^{-1} vertically downward, for a total velocity magnitude of 24.8 mm d^{-1}.

Filtering of the distance data

Velocities were calculated by first smoothing the distance measurements using a cubic-spline error-correction routine. Smoothing proceeded by assuming that a certain percentage of the root-mean-square deviation from a constant velocity (linear change in distance with time) was error. The percentage error was tuned by visually inspecting graphs, such as those in Figure 3, to determine when measurement-to-measurement variations had been damped without obscuring longer-term trends in the curves. Two goals of the smoothing were to make the smoothed curve stay within the range of the actual data over periods of several hours, while smoothing sufficiently to eliminate zero or negative speeds. Only round-number percentage errors (e.g. 20, 30%, etc.) were tried to prevent over-tuning of a somewhat arbitrary parameter. The procedure worked best on continuous periods of record, so the remaining discussion concentrates on three periods for which measurements were made with little interruption.

For the 412 measurements between 26 and 29 June (Fig. 3a) and the 404 measurements between 30 June and 3 July (Fig. 3b), smoothing was accomplished by assuming that 30% of the measurement variance was error. The greater noisiness of the 465 measurements made during 8–12 July (Fig. 3c) required assuming 40% of the measurement variance was in error in order to eliminate negative velocities. It is possible, particularly in this case, that some real results have been eliminated by oversmoothing. Amplitudes of the velocity variations depend strongly on the error-correction percentage chosen but the timing and phase of the cycles are unaffected. Values and first derivatives of the smoothed splines were calculated at 0.02 d intervals (~half-hourly). Velocities shown in Figure 3 and discussed here are the component of velocity from the prism towards the EDM, uncorrected for the true motion determined by the theodolite measurements.

For comparison with the measurements near the

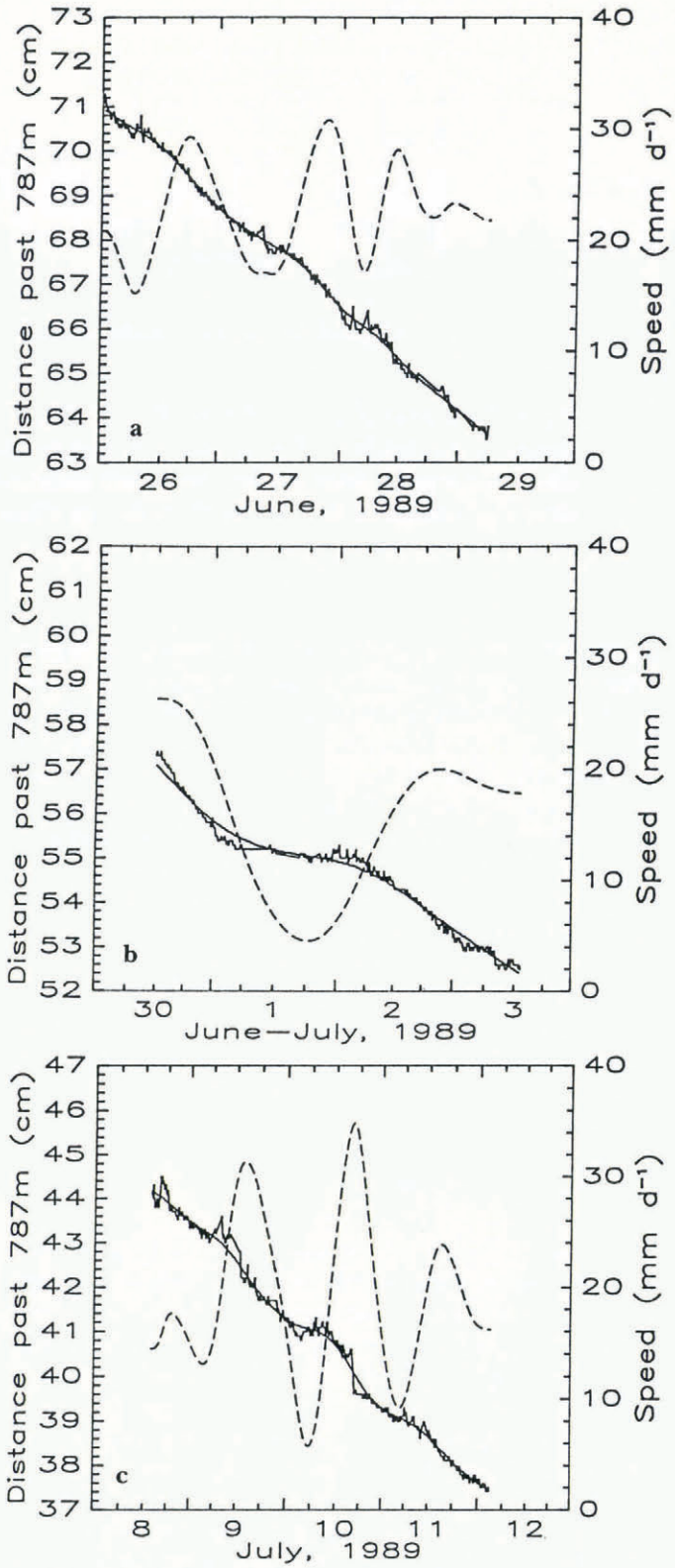

Fig. 3. Results of ADM measurements. Saw-tooth curves show measured distances from ADM to stake S30. Smooth solid curve is cubic-spline fit to these measurements. Dashed curve is resulting velocity. a. 26–29 June. b. 30 June–3 July. c. 8–12 July.

bergschrund, the movement of two stakes in the upper part of the ablation area was monitored daily (Fig. 4). Horizontal angles and distances were measured to these stakes. Also shown in Figure 4 are the rainfall and melt rate over the time interval between surveys. The latter was obtained by measuring heights of the stakes. There is

https://doi.org/10.3189/S0022143000003804 Published online by Cambridge University Press

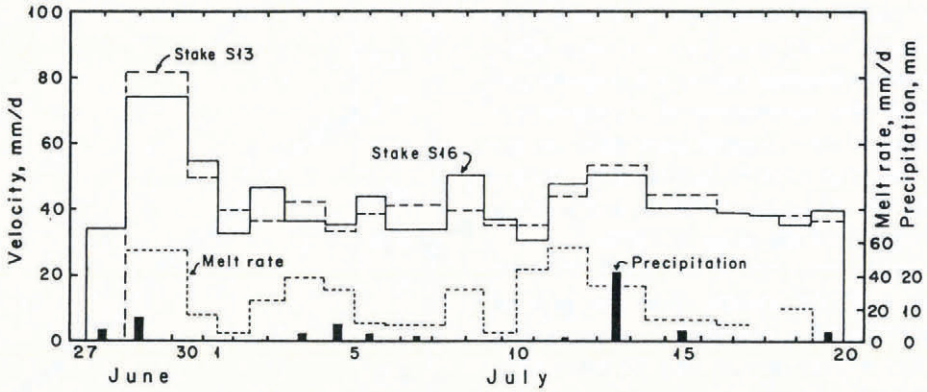

Fig. 4. Time series of velocity of stakes S13 and S16, of snowmelt between successive surveys (uncorrected for density changes) and of rainfall at Tarfala Station. Surveys were taken daily except when interrupted by weather. Summer snow-density measurements taken at other times on this glacier have been roughly constant at about 0.6 Mg m^{-3}. Timing and duration of rainfall events is not known, so bars are placed at mid-points between surveys.

good qualitative correlation between periods of higher water input (melt and rainfall) and increases in velocity.

A spectral-filtering calculation of velocity, similar to that used by Walters and Dunlop (1987), was also applied to the distance data. A Fast Fourier Transform performed on gridded, detrended data produced a periodogram showing moderate peaks at a frequency of 1 d^{-1} and at a possible harmonic of 1.8 d^{-1}, but the apparent noise frequencies have a power of similar, although smaller, magnitude. Digital filtering of a data set that is short compared to the most important frequency, and which has high noise levels, tended to produce velocities whose frequency of variations closely matched the cut-off frequency of filtering. We infer that the greater speeds considered by Walters and Dunlop (1987) would reduce the difficulties.

Interpretation of the data

Mean daily velocities of the stake near the bergschrund typically did not vary much from the ~20 mm d^{-1} average over the total measurement period. Variations on time-scales less than a day fall into three types: between 26 and 29 June (Fig. 3a) there are small cyclic, diurnal variations; from 30 June through 3 July (Fig. 3b) there is a significant non-diurnal variation over the entire period; and from 8 through 12 July there are large diurnal cycles (Fig. 3c). Diurnal cycles imply that the glacier responds, as expected, to water inputs that vary with daily temperature. Lagged correlations of velocity versus temperature indicated that the velocity maxima occur ~4.3 h after the daily temperature maxima, with daily temperature maxima at about 1500 h local time. (The maximum correlation was 0.47.)

Different weather was responsible for the two different types of diurnal cycle. 26–29 June was characterized by clouds, mild diurnal temperature cycles in the range −1°C to +8°C and occasional light rains. 8–12 July had virtually cloudless afternoons with 12 afternoon temperatures and intense radiation on the cirque headwall, leading nearly constantly to small avalanches. The raw distance data for these two periods (Fig. 3a and c) suggest that the radiative heating and associated near-surface air turbulence may have led to more measurement-to-measurement variability during the later period. A more stringent smoothing applied to data during such periods could probably be justified and would lead to a smaller diurnal cycle. Such smoothing would not obscure the essential result, which is that a larger diurnal velocity cycle results from a larger diurnal temperature cycle, presumably with increased meltwater input as the linking variable.

Besides meltwater, precipitation provides water input to the glacier. Rainfall was not measured in the cirque but daily totals were recorded at Tarfala Station (Fig. 4). Such measurements cannot be used to study details of the timing of the glacier's response to precipitation inputs because precipitation has a highly local character in mountainous areas. Furthermore, the EDM cannot take measurements in moderate rain and, because of lingering fog, EDM measurements do not provide reliable information on the time that rainfall ceased on the glacier. Thus, relations between rainfall and velocity changes must be inferred from the qualitative knowledge that rainfall occurred and the quantitative knowledge of distances before and after a rainfall event.

The velocity pattern during 30 June through 3 July (Fig. 3b) can probably be explained by rainwater inputs to the cirque. Heavy rains occurred during the morning of 29 June, preventing data collection. When measurements were resumed at midday on 30 June, the motion during the preceding day implied a velocity in excess of 50 mm d^{-1}. (A problem with the mounting bracket for the EDM required that it be dismounted, without moving its tripod, during this period. Even allowing for an inadvertant change of position of 1 cm or more, the position on 30 June implies the highest sustained speed during the experiment.) This velocity peak corresponds with the highest velocity peak recorded on stakes S13 and S16 (Fig. 4). After these high velocities, stake S30 underwent a rapid deceleration to nearly zero velocity (Fig. 3b). The raw-distance data actually show a slight negative velocity over a period of about 6 h near midnight on 1 July (Fig. 3b), suggesting that the bergschrund may have opened appreciably during the acceleration and ice was now settling back against the headwall.

https://doi.org/10.3189/S0022143000003804 Published online by Cambridge University Press

MODELING

Experiments with basal decoupling

We investigated the relation between basal-stress coupling and surface-velocity fluctuations using a two-dimensional steady-state finite-element program, described by Hanson (1990). The flowline simulated was approximately along the glacier center line, extending 3300 m from the bergschrund near stake S30 (Fig. 1) to the snout. This finite-element program uses convex quadrilateral elements, each defined by four nodes with linear variation assumed between adjacent nodes ("Taig quadrilaterals"; Irons and Ahmad, 1980). The grid used in these simulations contained elements arranged in a topologically rectangular array, with 165 columns, containing 16 elements, each 20 m wide. Vertical thicknesses of the elements varied, being 3 m in basal elements and increasing linearly with height at a rate controled by the thickness of the glacier in each column. Surface and bed profiles for the flowline were constructed from maps of the glacier surface (Holmlund and Schytt, 1987) and bed (Eriksson, 1990). Shape factors, ice viscosities, transverse strain rates and sliding velocities were varied within reasonable limits until calculated and measured surface velocities were in approximate agree-

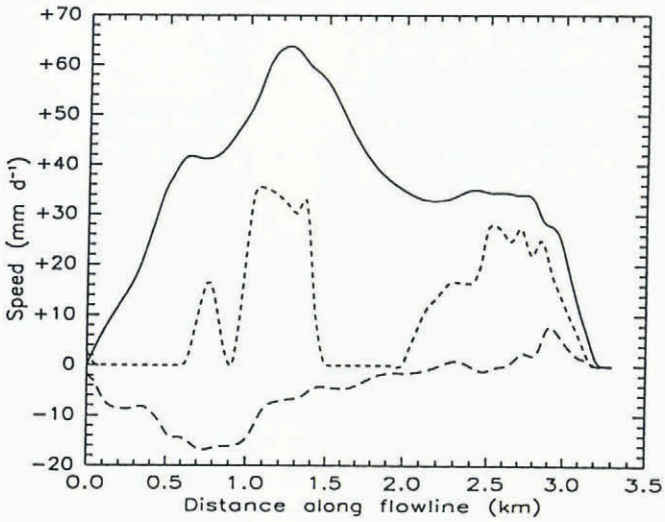

Fig. 5. Surface and basal velocity components from the model control run. Surface velocities are model results: solid curve is surface horizontal velocity and long-dashed curve is surface vertical velocity. Basal horizontal velocity (short-dashed curve) is the applied boundary condition.

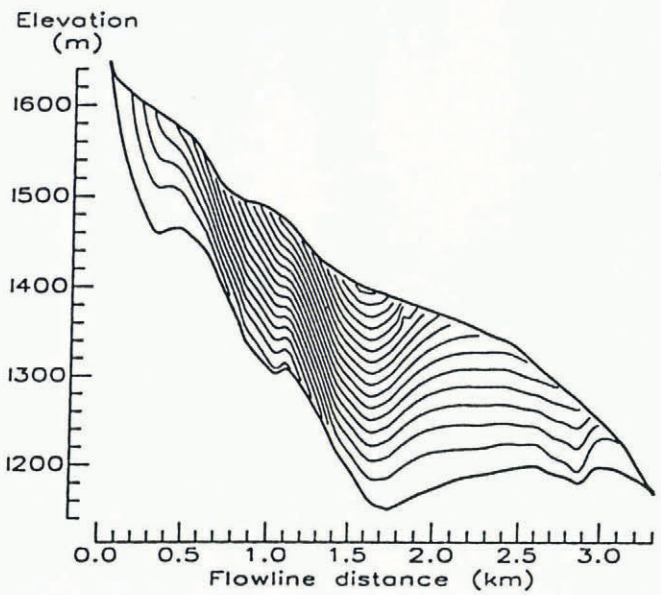

Fig. 6. Streamlines of the model control-run flow, shown as evenly spaced contours of a stream function, so that flow is faster where streamlines are closer together. Vertical exaggeration is approximately 5 : 1.

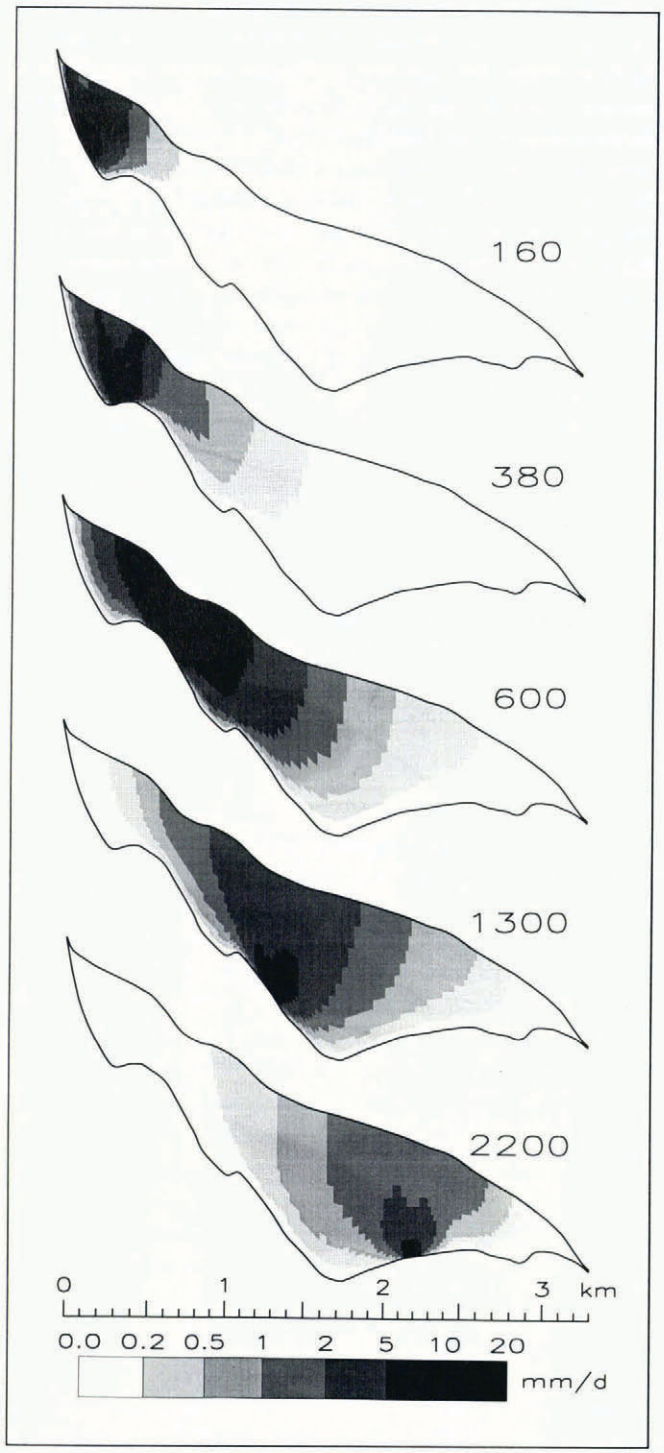

Fig. 7. Increases in velocity relative to the control run in five perturbation experiments. Centers of the 80 m wide decoupled zones are (top to bottom) 160, 380, 600, 1300 and 2200 m from the headwall.

https://doi.org/10.3189/S0022143000003804 Published online by Cambridge University Press

ment. The modeled flow pattern (Figs 5 and 6) will be used as a control run. All subsequent results are presented as deviations from the control run.

Perturbation experiments were performed by changing boundary conditions over short sections of the bed. In the control run, two specified velocity components fix the velocity at each basal node. In the decoupled zone of a perturbation experiment, the basal velocities are free in magnitude but constrained to follow the bed. No retarding stress is applied to the decoupled nodes in these experiments, so the simulated ice slides along a frictionless bed.

In the first series of simulations, a zone of five adjacent basal nodes was decoupled, leading to an 80 m zone of free sliding. This zone was bounded up- and down-glacier by 20 m zones of linear transition back to the control-run boundary conditions. Each simulation in the series had a decoupled zone in a different location, with the locations chosen for their varying basal topography. Distances from the headwall to the center point of decoupling are used to characterize the runs. The five zones in this series were: 160 m (at the lower headwall), 380 m (rising out of the first overdeepening), 600 m (descending out of the cirque after the first overdeepening), 1300 m (descending into the main overdeepening) and 2200 m (climbing the riegel out of the main overdeepening) (Fig. 7).

The responses to basal decoupling were similar in all five of the first series of experiments. In all cases, the surface horizontal velocity change was greater both up-glacier and down-glacier from the center of the basal perturbation than it was over the center (Fig. 8; Table 1). The two peaks were typically of the same magnitude, with the velocity near the center being one-third to two-thirds of the maximum. Vertical velocities dropped sharply on the up-glacier side of the perturbation and increased on the down-glacier side. Within each experiment, surface vertical-velocity changes were similar to, or slightly smaller than, the horizontal velocity changes.

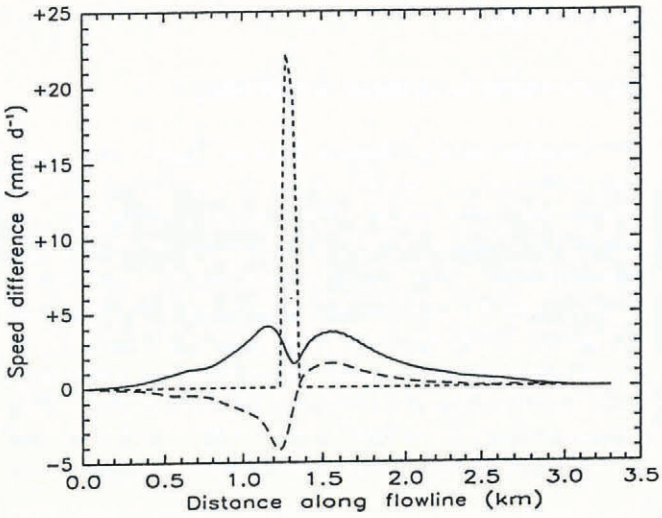

Fig. 8. Increases in velocity relative to the control run of surface and basal velocity components for an 80 m wide decoupled zone centered 1300 m from the headwall. The solid curve is surface-horizontal velocity; the long-dashed curve is surface-vertical velocity, and the short-dashed curve is basal horizontal velocity.

The pattern of vertical velocity response is forced by mass continuity and longitudinal strain rates near the base. Using x and z as horizontal and vertical coordinates, respectively, and u and w as the corresponding horizontal and vertical velocities, the decoupled zone near the bed produces a sharp increase in $\partial w/\partial x$, resulting from up-glacier extension and down-glacier compression. Since there is no change in glacier shape between the control run and the perturbation runs, the model maintains a roughly constant shear-stress pattern.

Table 1. Velocity responses for finite-element model perturbation experiments. The magnitude of each response is given in mm d^{-1}, and the displacement from the center of the perturbation (in parentheses) is given in meters. u_s^- is the surface-horizontal velocity at the up-glacier peak response point; u_s^0 is the surface-horizontal velocity at the minimum between the two peaks; u_s^+ is the surface-horizontal velocity at the down-glacier peak response point; w_s^- is the surface-vertical velocity response at the largest negative up-glacier point; w_s^+ is the surface-vertical velocity at the largest positive down-glacier point; and u_b is the basal horizontal-velocity peak response. All responses are differences from the control run

Center of decoupled zone	*Width of decoupled zone*	u_s^-	u_s^0	u_s^+	w_s^-	w_s^+	u_b
160	80	3.0 (−80)	1.3 (20)	3.6 (140)	−5.1 (−60)	2.0 (120)	12.2 (20)
380	80	5.0 (−140)	2.3 (0)	6.3 (120)	−4.8 (−140)	4.8 (100)	25.1 (20)
600	80	13.5 (−120)	9.3 (0)	14.3 (120)	−10.5 (−80)	3.2 (100)	54.1 (−20)
1300	80	4.1 (−140)	1.6 (20)	3.8 (240)	−4.2 (−60)	1.6 (260)	22.2 (−20)
2200	80	1.9 (−200)	1.0 (−20)	2.1 (160)	−1.4 (−100)	2.0 (80)	13.9 (−20)
1300	160	10.3 (−160)	6.0 (20)	9.6 (240)	−8.9 (−80)	4.1 (260)	34.3 (−20)
2200	160	5.6 (−200)	4.0 (−20)	6.3 (160)	−3.3 (−140)	4.3 (100)	22.8 (−60)
1300	240	19.8 (−160)	15.4 (60)	19.1 (240)	−15.2 (−100)	8.3 (260)	50.4 (−20)
2200	240	11.0 (−240)	9.2 (−60)	12.5 (200)	−5.4 (−180)	6.6 (120)	32.4 (−60)

https://doi.org/10.3189/S0022143000003804 Published online by Cambridge University Press

In particular, τ_{zz} remains constant, implying through the flow law that $\epsilon_{zz} = \frac{1}{2}(\partial u/\partial z + \partial w/\partial x)$ must also remain constant. The increase in $\partial w/\partial x$ must therefore be balanced by a decrease in $\partial u/\partial z$, producing a smaller increase in u at the surface.

Central depression of the surface horizontal velocity response is a robust feature of this type of experiment. It appears in various experiments not discussed here, such as with directly specified basal velocity changes and with idealized "slab" glacier geometries. Balise and Raymond (1985) found a similar response using an analytical solution of linear rheology, responding to a Gaussian spike of basal-velocity perturbation in an idealized slab solution. One would not necessarily expect a two-peak velocity response to appear in actual field data, primarily because basal lubrication would be expected to occur over a wider area and in multiple areas. Velocity data from the Large Stake Net experiment carried out on Storglaciären from 1984 through 1986 (Hooke and others, 1989) can be re-interpreted as having velocity-increase events with two separated maxima. This would be consistent with force-balance calculations suggesting that the principal area of reduction in basal drag was between the two peaks. However, we cannot separate the effects of glacier geometry on the velocity response from this theoretical stress-balancing process for the real data.

Interpretation of the model results

Individual experiments described here do not represent an actual event but rather serve as a mechanism for exploring the response of one part of the glacier to a point perturbation in another part of the glacier, conceptually similar to a Green's function. Diurnal-velocity variations were of comparable magnitude in both measured data and model perturbation responses. However, during an actual precipitation or high melt-rate event, large areas of the glacier bed would be undergoing at least a partial decoupling, so the measured responses within the cirque basin could in theory be some sort of non-linear sum over all of these model simulations.

Among perturbation experiments with the same-sized zone of basal decoupling, responses varied substantially both in magnitude of surface response (Table 1) and in longitudinal distance over which the decoupling had an influence (Fig. 7). Maximum surface magnitude and longitudinal coupling distance were not necessarily correlated—compare particularly the 600 and 1300 m experiments. The cirque appears to be the most isolated region of the glacier, as large responses from forcing within the cirque did not extend much beyond the first riegel, and large responses to forcing just below the cirque at 600 m propagated well down into the ablation zone. Heavy crevassing on the actual glacier at 350–550 m from the headwall along this flowline shows the relative independence of the cirque from the rest of the glacier. Responses at 600 m may be exaggerated, however, because initial tuning suggests that the glacier has negligible sliding speeds over the highest riegel. Hence, complete decoupling here actually constituted the greatest decrease in inferred basal stress. Responses to decoupling centered at 500 m (not shown) were somewhat smaller and responses to experiments centered at 700 m (not shown) were much smaller.

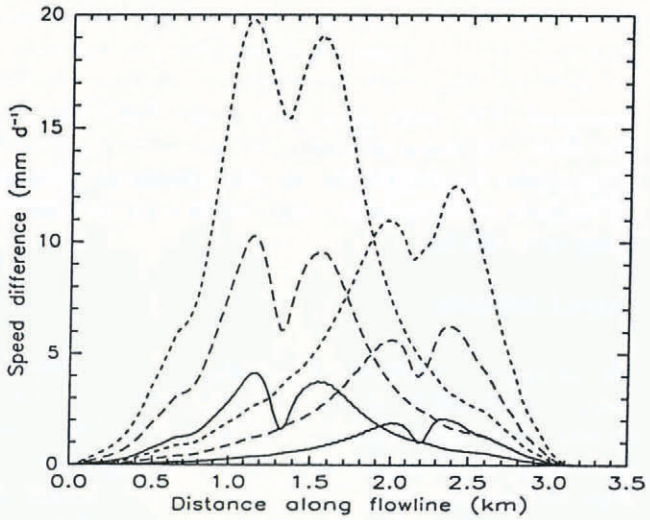

Fig. 9. Responses of surface-horizontal velocity to various widths of the zone of basal decoupling. Widths of decoupling are 80, 160 and 240 m, centered at 1300 and 2200 m from the headwall.

Basal accelerations in the zone of descent into the main overdeepening (1300 m) produced the greatest horizontal extent of response. Both the magnitude of this response and its extent were roughly double those of perturbations at 2200 m. Additional experiments at 1300 and 2200 m were run to explore the effect of the size of the decoupled zone on the results. At each location, the model was run with 160 m wide and 240 m wide zones of decoupling (Table 1; Fig. 9). At both locations, in response to a doubled zone of decoupling, the basal response was slightly less than doubled and the surface response was more than doubled. With 240 m of decoupling centered at 1300 m, the response in excess of 0.2 mm d^{-1} extended well up into the cirque. We conclude from these results that the response of a glacier to decoupling in a number of areas would be non-linear, rather than a simple sum of individual experiments.

Model results clearly suggest that observed velocity variations within the cirque have resulted from basal decoupling either within the cirque or just below it. The short lag of a few hours between maximum temperature and maximum velocity further suggests that the bergschrund was the major point of meltwater input. The crevasse zone below the cirque remained covered with the previous winter's snow throughout the period of measurements, so all water inputs there would have required a period of percolation. Even though the greatest water inputs and velocity variations occur much lower on the glacier, the longitudinal traction from the main overdeepening does not extend back into the cirque. The correlation between velocities in the cirque and velocities measured at a coarser time resolution in the ablation zone reflects the fact that Storglaciären is small from a micrometeorological point of view. A weather event leading to high water inputs (either by melting or precipitation) will typically cover the whole glacier simultaneously.

Model results cannot further refine the position of basal decoupling. Perturbations using a completely

https://doi.org/10.3189/S0022143000003804 Published online by Cambridge University Press

decoupled zone 80 m long are a numerically convenient proxy for the more complicated character of actual water-pressure events, which presumably produce partial decoupling over large parts of a glacier bed. The fact that 80 m decoupling produced surface-velocity changes comparable in magnitude to the measured diurnal fluctuations does not imply that this is what is actually going on at the bed.

CONCLUSIONS

The principal conclusion of this study is that diurnal velocity fluctuations of up to three times the mean velocity occur even high in a cirque. Presumably, these fluctuations are driven by a partial decoupling of the ice from its bed resulting from water inputs. Modeling suggests that the region of decoupling must be within or just below the cirque. Consideration of both the modeling and the short lag between temperature fluctuations and velocity fluctuations suggests that the bergschrund is the most important point of water input.

ACKNOWLEDGEMENTS

This research was financed by the U.S. National Science Foundation (grants DPP-8619086, INT-8712749 and DPP-8822156), the Swedish Natural Sciences Research Council and the University of Delaware Research Foundation.

REFERENCES

Balise, M.J. and C.F. Raymond. 1985. Transfer of basal sliding variations to the surface of a linearly viscous glacier. *J. Glaciol.*, **31**(109), 308–318.

Eriksson, M. 1990. Storglaciärens bottentopografi uppmätt genom radioekosondering. (Examensarbete, University of Stockholm. Department of Physical Geography.)

Hanson, B. 1990. Thermal response of a small ice cap to climatic forcing. *J. Glaciol.*, **36**(122), 49–56.

Holmlund, P. and V. Schytt. 1987. *Glaciärerna i Tarfala.* [Map.] Stockholm, University of Stockholm. Department of Physical Geography.

Hooke, R. LeB., P. Calla, P. Holmlund, M. Nilsson and A. Stroeven. 1989. A 3 year record of seasonal variations in surface velocity, Storglaciären, Sweden. *J. Glaciol.*, **35**(120), 235–247.

Iken, A. and R.A. Bindschadler. 1986. Combined measurements of subglacial water pressure and surface velocity of Findelengletscher, Switzerland: conclusions about drainage system and sliding mechanism. *J. Glaciol.*, **32**(110), 101–119.

Irons, B.M. and S. Ahmad. 1980. *Techniques of finite elements.* New York, John Wiley and Sons.

Jansson, P. and R. LeB. Hooke. 1989. Short-term variations in strain and surface tilt on Storglaciären, Kebnekaise, northern Sweden. *J. Glaciol.*, **35**(120), 201–208.

Kamb, W.B. and K.A. Echelmeyer. 1986. Stress-gradient coupling in glacier flow: I. Longitudinal averaging of the influence of ice thickness and surface slope. *J. Glaciol.*, **32**(111), 267–284.

Walters, R.A. and W.W. Dunlap. 1987. Analysis of time series of glacier speed: Columbia Glacier, Alaska. *J. Geophys. Res.*, **92**(B9), 8969–8975.

The accuracy of references in the text and in this list is the responsibility of the authors, to whom queries should be addressed.

MS received 17 January 1992 and in revised form 21 July 1992

https://doi.org/10.3189/S0022143000003804 Published online by Cambridge University Press